Computer Modeling in Engineering & Sciences

Tech Science Press

DOI: 10.32604/cmes.2022.019154

ARTICLE

Efficient Numerical Scheme for the Solution of HIV Infection $CD4^+$ T-Cells Using Haar Wavelet Technique

Rohul Amin[1], Şuayip Yüzbaşı[2,*] and Shah Nazir[3]

[1]Department of Mathematics, University of Peshawar, Peshawar, 25120, Pakistan

[2]Department of Mathematics, Faculty of Science, Akdeniz University, Antalya, Tr-07058, Turkey

[3]Department of Computer Science, University of Swabi, Swabi, 23430, Pakistan

[*]Corresponding Author: Şuayip Yüzbaşı. Email: suayipyuzbasi@gmail.com

Received: 06 September 2021 Accepted: 05 November 2021

ABSTRACT

In this paper, Haar collocation algorithm is developed for the solution of first-order of HIV infection $CD4^+$ T-Cells model. In this technique, the derivative in the nonlinear model is approximated by utilizing Haar functions. The value of the unknown function is obtained by the process of integration. Error estimation is also discussed, which aims to reduce the error of numerical solutions. The numerical results show that the method is simply applicable. The results are compared with Runge-Kutta technique, Bessel collocation technique, LADM-Pade and Galerkin technique available in the literature. The results show that the Haar technique is easy, precise and effective.

KEYWORDS

System of nonlinear differential equations; HIV infection of $CD4^+$ T-cells; Broyden method; Haar wavelet; residual error estimation

1 Introduction

Many models have been developed by mathematicians in the last decade to explain the immunological response to Human Immunodeficiency Virus (HIV) infection. Due to the scarcity of $CD4^+$ T-cells, HIV disease is considered to result in concealment of the immune system (referred to generally as T4-cells or T-helper cells), cells which play a focal part in the human immune system. A class of white blood cells called $CD4^+$ T-cells is essentially infected by HIV and this selective depletion of $CD4^+$ T-cells means that a focal part in the resistant direction fills in as a clinical marker to estimate HIV disease movement. Mathematical models play an important role in the dynamics of these infectious diseases [1–6]. The level of $CD4^+$ T-cells in the fringe blood is controlled at a level between 800 and 1200 mm^{-3} in a normal human body. These cells are the most inexhaustible white blood cell of the human safe framework, which battle against diseases [7]. Many authors introduced different numerical methods for the investigation of $CD4^+$ T-cells [8–14].

In recent years, many researchers have studied on new analytical and numerical methods for model problems characterized by differential equations. Yüzbaşi et al. [15] presented the Pell–lucas collocation method for the solutions of two population models and residual correction. Mallawi et al. [16] utilized Legendre collocation method to the space–time variable fractional-order advection–dispersion equation. Yüzbaşi [17] used an operational method for solutions of Riccati type differential equations. Chu et al. [18] studied the generalized $(2+1)$ dimensional shallow water equation. The solution for the fractional system of HIV-1 infection of $CD4^+$ T-cells was studied by Khater et al. [19] by using Atangana–Baleanu fractional derivative. Khater et al. [20] developed a semi analytical and numerical scheme for a biological model. Khater et al. [21] used the trigonometric quintic B-spline technique for the solutions of complex nonlinear Fokas–Lenells equations. In reference [22] the nonlinear phi-four equation is solved through two analytical and semi-analytical techniques. Khater et al. [23] used trigonometric Quintic B-spline method for the solution of conformable fractional nonlinear time-space telegraph equation. Khater et al. [24] investigated the analytical and numerical solutions of the modified Benjamin–Bona–Mahony equation via the modified B–spline collection method. Khater et al. [25] found the solution of nonlinear Klein–Fock–Gordon equation by using generalized exponential function and generalized Riccati expansion methods. Khater et al. [26] investigated the analytical and semi-analytical solutions of the time-fractional Cahn–Allen equation by using the Adomian decomposition method. Khater et al. [27] found the analytical solutions of the nonlinear Schrodinger equation with the higher-order through Kudryashov method. They also found the solutions of quadratic cubic fractional nonlinear Schrodinger equation by Adomian decomposition process [28]. Khater et al. [29] used the trigonometric quintic and exponential cubic B-spline schemes for the solutions of the nonlinear Klein-Gordon-Zakharov model. Yue et al. [30] found a solution of the fractional nonlinear Hirota–Satsuma–Shallow water wave equation by using a modified Kudryashov method. Khater et al. [31] found solutions of the Fisher-Kolmogorov-Petrovskii-Piskunov model by employing the modified Kudryashov and trigonometric-quantic B-spline methods. Li et al. [32] found wave solutions of the $(2+1)$ dimensional Kadomtsev Petviashvili Benjamin Bona Mahony model. Smadi et al. [33] study the accuracy of solution for fractional order an SEIR epidemic model by using the homotopy analysis method. Freihet et al. [34] found a solution of a fractional stiff system using residual functions algorithm. Smadi et al. [35] developed analytical technique for coupled system of fractional partial differential equations, for solutions of nonlinear fractional Kundu-Eckhaus equations [36] and for solution of coupled fractional resonant Schrodinger equations [37]. The same authors analyzed and investigated the analytical solution of the seventh-order fractional Sawada Kotera Ito, Lax, and Kaup Kupershmidt equations [38]. Moreover, the authors also analyzed and studied fuzzy fractional differential equations in terms of Atangana-Baleanu Caputo differential operators equipped with uncertain constraints coefficients and initial conditions [39].

Here we develop an accurate scheme by using HWC technique for the solution of the HIV infection of $CD4^+$ T-cells. The main contributions of this work as:

- To develop efficient numerical scheme by utilizing HWC technique for HIV infection $CD4^+$ T-cells
- To design numerical scheme using HWC technique
- To evaluate the efficacy of the established technique in some instances and compare the results with other techniques Runge-Kutta, LADM-Pade [1], Bessel collocation technique [2], PIA(1,1) [3], MVIM [4], DTM [7] and Galerkin technique [5] available in the literature

In this article we find the numerical solution of first order model of the form [5]

$$\begin{cases} \dfrac{dT}{dt} = \lambda - \alpha T + rT\left(1 - \dfrac{T+I}{T_{\max}}\right) - k^* VT, \\ \dfrac{dI}{dt} = k^* VT - \beta I, \\ \dfrac{dV}{dt} = N^* \beta I - \gamma V, \end{cases} \tag{1}$$

with initial conditions:

$$T(0) = T_0, \quad I(0) = I_0 \quad \text{and} \quad V(0) = V_0. \tag{2}$$

Here $T(t)$, $I(t)$, $V(t)$ are used for concentration of uninfected cells, infected cells and free virus particles of $CD4^+$ T-cells by HIV in the blood. $rT\left(1 - \frac{T+I}{T_{\max}}\right)$ is logistic growth of the healthy cells, $T_{\max}$ is the most extreme level of cells in the human body, k is the steady rate which the body produces cells, k^*VT is the frequency of HIV infection of healthy cells, $k^* > 0$ is the rate of virus infection, $N^*\beta$ is the rate of virus production by contaminated cells, where N^* is the average number of particles of infection produced by the infected T-cell, and γ is the rate of death of particles of the virus.

The paper is structured as: In Section 2, Haar functions are defined. HWC technique for solution of HIV infection is given in Section 3. In Section 4 error estimation about the model is given. In Section 5, one example is given. Conclusion is given in the last Section 6.

2 Haar Wavelet

Here we discuss Haar functions, integration of Haar functions and collocation points.

Definition 2.1. Scaling function on $[\alpha_1, \alpha_2)$ is [40]

$$h_1(t) = \begin{cases} 1 & \text{for } t \in [\alpha_1, \alpha_2), \\ 0 & \text{elsewhere.} \end{cases} \tag{3}$$

Mother wavelet on $[\alpha_1, \alpha_2)$ is

$$h_2(t) = \begin{cases} 1 & \text{for } t \in \left[\alpha_1, \dfrac{\alpha_1 + \alpha_2}{2}\right), \\ -1 & \text{for } t \in \left[\dfrac{\alpha_1 + \alpha_2}{2}, \alpha_2\right), \\ 0 & \text{elsewhere.} \end{cases} \tag{4}$$

The other terms can be written as

$$h_i(t) = \begin{cases} 1 & \text{for } t \in [\eta_1, \eta_2), \\ -1 & \text{for } t \in [\eta_2, \eta_3), \\ 0 & \text{elsewhere,} \end{cases} \tag{5}$$

where $\eta_1 = \alpha_1 + (\alpha_2 - \alpha_1)\frac{\zeta}{d}, \eta_2 = \alpha_1 + (\alpha_2 - \alpha_1)\frac{\zeta+0.5}{d}, \eta_3 = \alpha_1 + (\alpha_2 - \alpha_1)\frac{\zeta+1}{d}$, where $d = 2^r$, and $r = 0, 1, \ldots, d-1$. If we take interval $[0, 1]$, then values of η_1, η_2 and η_3 are: $\eta_1 = \frac{\zeta}{d}$, $\eta_2 = \frac{1/2+\zeta}{d}$, $\eta_3 = \frac{1+\zeta}{d}$. Any member $u(t)$ in $L^2[0, 1)$, is written as $u(t) = \sum_{k=1}^{\infty} \lambda_k h_k(t)$, we truncate this series is $u(t) \approx \sum_{k=1}^{N} \lambda_k h_k(t)$.

Using the notation

$$p_{i,1}(t) = \int_0^t h_i(x)dx, \tag{6}$$

and

$$p_{i,1}(t) = \begin{cases} t - \rho_1 & \text{for } t \in [\eta_1, \eta_2), \\ \eta_3 - t & \text{for } t \in [\eta_2, \eta_3), \\ 0 & \text{elsewhere.} \end{cases} \tag{7}$$

Generally,

$$p_{i,n}(t) = \int_0^t p_{i,n-1}(x)dx. \tag{8}$$

Thus $p_{i,n}(t)$ is obtained as under [40]

$$p_{i,n}(t) = \begin{cases} 0 & \text{for } t \in [0, \rho_1), \\ \dfrac{(t-\rho_1)^n}{n!} & \text{for } t \in [\rho_1, \rho_2), \\ \dfrac{[(t-\rho_1)^n - 2(\rho_1 - \rho_2)^n]}{n!} & \text{for } t \in [\rho_2, \rho_3), \\ \dfrac{1}{n!}\left[(t-\rho_1)^n - 2(\rho_1 - \rho_2)^n + (t-\rho_3)^n\right], & \text{for } t \in [\rho_3, 1). \end{cases} \tag{9}$$

Definition 2.2. The $[\beta_1, \beta_2]$ interval for HWC scheme is discretized as [40]

$$t_i = \beta_1 + (\beta_2 - \beta_1)\frac{i - 1/2}{2M} \quad i = 1, 2, 3, 4, \ldots, 2M = N. \tag{10}$$

In the above Eq. (10), a collocation point (CP) are defined. Some of the recent work using HWC technique can be seen in [41–47].

3 Numerical Method

The implementation of the HWC method is discussed in this section in order to find the HIV model solution provided in Eq. (1). Using Haar functions, the derivative of the unknown function in the method is approximated and the expression for the unknown function is obtained by using initial condition and integration. By applying the Haar technique to Eq. (1) and putting the CPs, we get a system of algebraic equations. The Broyden technique is used to find solution of this system. At last, the approximate solution at CPs is obtained using these coefficients. We use the symbols $\Theta_1 = \sum_{i=1}^{N}$ and $\Theta_2 = \sum_{i=1}^{M}$.

First, we consider that $T'(t)$, $I'(t)$ and $V'(t)$ are square integrable function and hence can be written as

$$T'(t)=\Theta_1 a_i h_i(t),\quad I'(t)=\Theta_1 b_i h_i(t)\quad \text{and}\quad V'(t)=\Theta_1 c_i h_i(t). \tag{11}$$

Integrating with respect to t, we have

$$T_N(t)=T_0+\Theta_1 a_i p_{i,1}(t),\quad I_N(t)=I_0+\Theta_1 b_i p_{i,1}(t),\quad \text{and}\quad V_N(t)=V_0+\Theta_1 c_i p_{i,1}(t). \tag{12}$$

Putting Eq. (11) and Eq. (12) in Eq. (1), we have

$$\begin{aligned}
\Theta_1 a_i h_i(t) &= \lambda-\alpha\left(T_0+\Theta_1 a_i p_{i,1}(t)\right)-k^*\left(v_0+\Theta_1 c_i p_{i,1}(t)\right)\left(T_0+\Theta_1 a_i p_{i,1}(t)\right)\\
&\quad +r\left(T_0+\Theta_1 a_i p_{i,1}(t)\right)\left[1-\frac{\left(T_0+\Theta_1 a_i p_{i,1}(t)\right)\left(I_0+\Theta_1 b_i p_{i,1}(t)\right)}{T_{\max}}\right],\\
\Theta_1 b_i h_i(t) &= k^*\left(v_0+\Theta_1 c_i p_{i,1}(t)\right)\left(T_0+\Theta_1 a_i p_{i,1}(t)\right)-\beta\left(I_0+\Theta_1 b_i p_{i,1}(t)\right),\\
\Theta_1 c_i h_i(t) &= N^*\beta\left(I_0+\Theta_1 b_i p_{i,1}(t)\right)-\gamma\left(V_0+\Theta_1 c_i p_{i,1}(t)\right),
\end{aligned}$$

by simplification we have

$$\begin{aligned}
&\Theta_1 a_i h_i(t)-\lambda+\alpha\left(T_0+\Theta_1 a_i p_{i,1}(t)\right)+k^*\left(v_0+\Theta_1 c_i p_{i,1}(t)\right)\left(T_0+\Theta_1 a_i p_{i,1}(t)\right)\\
&\quad -r\left(T_0+\Theta_1 a_i p_{i,1}(t)\right)\left[1-\frac{\left(T_0+\Theta_1 a_i p_{i,1}(t)\right)\left(I_0+\Theta_1 b_i p_{i,1}(t)\right)}{T_{\max}}\right]=0,\\
&\Theta_1 b_i h_i(t)-k^*\left(v_0+\Theta_1 c_i p_{i,1}(t)\right)\left(T_0+\Theta_1 a_i p_{i,1}(t)\right)+\beta\left(I_0+\sum_{i=1}^{N} b_i p_{i,1}(t)\right)=0,\\
&\Theta_1 c_i h_i(t)-N^*\beta\left(I_0+\Theta_1 b_i p_{i,1}(t)\right)+\gamma\left(V_0+\Theta_1 c_i p_{i,1}(t)\right)=0,
\end{aligned}$$

putting the CPs (10), we have

$$\begin{aligned}
F_{1,j} &= \Theta_1 a_i\ h_i(t)-\lambda+\alpha\left(T_0+\Theta_1 a_i p_{i,1}(t)\right)+k^*\left(v_0+\Theta_1 c_i p_{i,1}(t)\right)\left(T_0+\Theta_1 a_i p_{i,1}(t)\right)\\
&\quad -r\left(T_0+\Theta_1 a_i p_{i,1}(t)\right)\left[1-\frac{\left(T_0+\Theta_1 a_i p_{i,1}(t)\right)\left(I_0+\Theta_1 b_i p_{i,1}(t)\right)}{T_{\max}}\right],\\
F_{2,j} &= \Theta_1 b_i h_i(t)-k^*\left(v_0+\Theta_1 c_i p_{i,1}(t)\right)\left(T_0+\Theta_1 a_i p_{i,1}(t)\right)+\beta\left(I_0+\Theta_1 b_i p_{i,1}(t)\right)=0,\\
F_{3,j} &= \Theta_1 c_i h_i(t)-N^*\beta\left(I_0+\Theta_1 b_i p_{i,1}(t)\right)+\gamma\left(V_0+\Theta_1 c_i p_{i,1}(t)\right)=0.
\end{aligned}$$

This is solved by Broyden's method. Jacobian is

$$\mathbf{J}=[J_{jk}]_{3N\times 3N}, \tag{13}$$

where

$$J_{jk}=\begin{cases}\dfrac{\partial F_{1,j}}{\partial a_k}=h_k(t_j)+\alpha p_{k,1}(t_j)-rp_{k,1}(t_j)-k^*[V_0p_{k,1}(t_j)+\Theta_1c_ip_{i,1}(t_j)p_{k,1}(t_j)\\ \qquad\qquad +\dfrac{r}{T_{\max}}\left[(T_0+\Theta_1a_ip_{i,1}(t_j))2p_{k,1}(t_j)+I_0p_{k,1}(t_j)+p_{k,1}(t_j)\Theta_1c_ip_{i,1}(t_j)\right],\\ \dfrac{\partial F_{1,j}}{\partial b_k}=T_0p_{k,1}(t_j)+\Theta_1a_ip_{i,1}(t_j)p_{k,1}(t_j),\\ \dfrac{\partial F_{1,j}}{\partial c_k}=-k^*T_0p_{k,1}(t_j)+\Theta_1a_ip_{i,1}(t_j)p_{k,1}(t_j),\\ \dfrac{\partial F_{2,j}}{\partial a_k}=-k^*V_0p_{k,1}(t_j)\left(1+\Theta_1p_{k,1}(t_j)\right),\\ \dfrac{\partial F_{2,j}}{\partial b_k}=h_k(t_j)+\beta p_{k,1}(t_j),\\ \dfrac{\partial F_{2,j}}{\partial c_k}=-k^*I_0p_{k,1}(t_j)\left(1+\Theta_1p_{k,1}(t_j)\right),\\ \dfrac{\partial F_{3,j}}{\partial a_k}=0,\\ \dfrac{\partial F_{3,j}}{\partial b_k}=-N^*\beta p_{k,1}(t_j),\\ \dfrac{\partial F_{3,j}}{\partial c_k}=h_k(t_j)+\gamma p_{k,1}(t_j).\end{cases}$$

The solution of this gives the values of unknown coefficients a_i's, b_i's and c_i's. The required solution $T_N(t)$, $I_N(t)$ and $V_N(t)$ at CPs is calculated by putting a_i, b_i c_i's in Eq. (12).

4 Error Estimation

Here, we study the residual error estimation [5] for HIV model (1) utilizing HWC technique. The residual functions $R_{1,N}(t)$, $R_{2,N}(t)$ and $R_{3,N}(t)$ are

$$\begin{cases}R_{1,N}(t)=T'_N-\lambda+\alpha T_N-rT_N\left(1-\dfrac{T_N+I_N}{T_{\max}}\right)+k^*V_NT_N,\\ R_{2,N}(t)=I'_N-k^*V_NT_N+\beta I_N,\\ R_{3,N}(t)=V'_N-N^*\beta I_N+\gamma V_N,\end{cases}\tag{14}$$

Define the error function as

$$\begin{cases}e_{1,N}(t)=T(t)-T_N(t),\\ e_{2,N}(t)=I(t)-I_N(t),\\ e_{2,N}(t)=V(t)-V_N(t),\end{cases}\tag{15}$$

where $T(t)$, $I(t)$ and $V(t)$ are exact solutions. So, we have

$$\begin{cases}T(t)=e_{1,N}(t)+T_N(t),\\ I(t)=e_{2,N}(t)+I_N(t),\\ V(t)=e_{3,N}(t)+V_N(t).\end{cases}\tag{16}$$

Also, we can write

$$\begin{cases} T'(t) - T'_N(t) = [T(t) - T_N(t)]' = \left[e_{1,N}(t)\right]' \\ I'(t) - I'_N(t) = [I(t) - I_N(t)]' = \left[e_{2,N}(t)\right]' \\ V'(t) - V'_N(t) = [V(t) - V_N(t)]' = \left[e_{3,N}(t)\right]'. \end{cases} \tag{17}$$

By subtracting system (14) from system (1), we have

$$\begin{cases} T'(t) - T'_N(t) = -\alpha\,[T(t) - T_N(t)] + r\,[T(t) - T_N(t)] - \dfrac{r}{T_{\max}}\Big[T^2(t) - T_N^2(t) + T(t)I(t) \\ \qquad\qquad -T_N(t)I_N(t)] - k^*\,[V(t)T(t) - V_N(t)T_N(t)] - R_{1,N}(t), \\ I'(t) - I'_N(t) = k^*\,[V(t)T(t) - V_N(t)T_N(t)] - \beta\,[I(t) - I_N(t)] - R_{2,N}(t), \\ V'(t) - V'_N(t) = N^*\beta\,[I(t) - I_N(t)] - \gamma\,[V(t) - V_N(t)] - R_{3,N}(t). \end{cases} \tag{18}$$

By using systems (5)–(6) in Eq. (7) and simplifying, we obtain

$$\begin{cases} \left[e_{1,N}(t)\right]' = -\alpha e_{1,N}(t) + r e_{1,N}(t) - \dfrac{r}{T_{\max}}\left[e_{1,N}^2(t) + e_{1,N}(t)e_{2,N}(t) + e_{1,N}(t)I_N + e_{2,N}(t)T_N\right] \\ \qquad\qquad -k^*\left[e_{1,N}(t)e_{3,N}(t) + e_{3,N}(t)T_N + e_{1,N}(t)V_N\right] - R_{1,N}(t), \\ \left[e_{2,N}(t)\right]' = k^*\left[e_{1,N}(t)e_{3,N}(t) + e_{3,N}(t)T_N + e_{1,N}(t)V_N\right] - \beta e_{2,N}(t) - R_{2,N}(t), \\ \left[e_{3,N}(t)\right]' = N^*\beta e_{2,N}(t) - \gamma e_{3,N}(t) - R_{3,N}(t). \end{cases} \tag{19}$$

where $e_{1,N}(t)$, $e_{2,N}(t)$ and $e_{3,N}(t)$ are unknowns functions. The initial conditions for approximate solution $T_N(t)$, $I_N(t)$ and $V_N(t)$ are

$$T_N(0) = T_0, \quad I_N(0) = I_0 \quad \text{and} \quad V_N(0) = V_0, \tag{20}$$

so initial conditions for system (19) are $e_{1,N}(0) = 0$, $e_{2,N}(0) = 0$ and $e_{3,N}(0) = 0$, where $e_{1,N}(t)$, $e_{2,N}(t)$ and $e_{3,N}(t)$ are estimated by $e_{1,N,M}(t)$, $e_{2,N,M}(t)$ and $e_{3,N,M}(t)$ the Haar wavelet technique.

Let $\left[e_{1,N,M}(t)\right]'$, $\left[e_{2,N,M}(t)\right]'$ and $\left[e_{3,N,M}(t)\right]'$ are in $L_2[0,1)$, so

$$\left[e_{1,N,M}(t)\right]' = \Theta_2 \xi_i h_i(t), \quad \left[e_{2,N,M}(t)\right]' = \Theta_2 \mu_i h_i(t) \quad \text{and} \quad \left[e_{3,N,M}(t)\right]' = \Theta_2 \nu_i h_i(t). \tag{21}$$

Integrating the above system (21), with respect to t we obtain the following expression:

$$e_{1,N,M}(t) = \Theta_2 \xi_i p_{i,1}(t), \quad e_{2,N,M}(t) = \Theta_2 \mu_i p_{i,1}(t), \quad \text{and} \quad e_{3,N,M}(t) = \Theta_2 \nu_i p_{i,1}(t). \tag{22}$$

Applying Haar approximations, we have

$$\begin{aligned} \Theta_2 \xi_i h_i(t) \;=\; & -\alpha \Theta_2 \xi_i p_{i,1}(t) - k^*\left[\Theta_2 \xi_i p_{i,1}(t)\Theta_2 \nu_i p_{i,1}(t) + T_N \Theta_2 \nu_i p_{i,1}(t) + V_N \Theta_2 \xi_i p_{i,1}(t)\right] \\ & - \frac{r}{T_{\max}}\left[\left(\Theta_2 \xi_i p_{i,1}(t)\right)^2 + \Theta_2 \xi_i p_{i,1}(t)\Theta_2 \mu_i p_{i,1}(t) + I_N \Theta_2 \xi_i p_{i,1}(t) + T_N \Theta_2 \mu_i p_{i,1}(t)\right] - R_{1,N}(t), \\ \Theta_2 \mu_i h_i(t) \;=\; & k^*\left[\Theta_2 \xi_i p_{i,1}(t)\Theta_2 \nu_i p_{i,1}(t) + T_N \Theta_2 \nu_i p_{i,1}(t) + V_N \Theta_2 \xi_i p_{i,1}(t)\right] - \beta \Theta_2 \mu_i p_{i,1}(t) - R_{2,N}(t), \\ \Theta_2 \nu_i h_i(t) \;=\; & N^* \beta \Theta_2 \mu_i p_{i,1}(t) - \gamma \Theta_2 \nu_i p_{i,1}(t) - R_{3,N}(t), \end{aligned}$$

After simplification, we have

$$F_{1,j}=\Theta_2\xi_i h_i(t)+\alpha\Theta_2\xi_i p_{i,1}(t)+k^*\left[\Theta_2\xi_i p_{i,1}(t)\Theta_2\nu_i p_{i,1}(t)+T_N\Theta_2\nu_i p_{i,1}(t)+V_N\Theta_2\xi_i p_{i,1}(t)\right]$$
$$+\frac{r}{T_{\max}}\left[\left(\Theta_2\xi_i p_{i,1}(t)\right)^2+\Theta_2\xi_i p_{i,1}(t)\Theta_2\mu_i p_{i,1}(t)+I_N\Theta_2\xi_i p_{i,1}(t)+T_N\Theta_2\mu_i p_{i,1}(t)\right]+R_{1,N}(t)=0,$$
$$F_{2,j}=\Theta_2\mu_i h_i(t)-k^*\left[\Theta_2\xi_i p_{i,1}(t)\Theta_2\nu_i p_{i,1}(t)+T_N\Theta_2\nu_i p_{i,1}(t)+V_N\Theta_2\xi_i p_{i,1}(t)\right]$$
$$+\beta\Theta_2\mu_i p_{i,1}(t)+R_{2,N}(t)=0,$$
$$F_{3,j}=\Theta_2\nu_i h_i(t)-N^*\beta\Theta_2\mu_i p_{i,1}(t)+\gamma\Theta_2\nu_i p_{i,1}(t)+R_{3,N}(t),$$

putting the discrete CPs (10), we obtain

$$F_{1,j}=\Theta_2\xi_i h_i(t_j)+\alpha\Theta_2\xi_i p_{i,1}(t_j)+k^*\left[\Theta_2\xi_i p_{i,1}(t_j)\Theta_2\nu_i p_{i,1}(t_j)+T_N\Theta_2\nu_i p_{i,1}(t_j)+V_N\Theta_2\xi_i p_{i,1}(t_j)\right]$$
$$+\frac{r}{T_{\max}}\left[\left(\Theta_2\xi_i p_{i,1}(t_j)\right)^2+\Theta_2\xi_i p_{i,1}(t_j)\Theta_2\mu_i p_{i,1}(t_j)+I_N\Theta_2\xi_i p_{i,1}(t_j)+T_N\Theta_2\mu_i p_{i,1}(t_j)\right]+R_{1,N}(t_j),$$
$$F_{2,j}=\Theta_2\mu_i h_i(t_j)-k^*\left[\Theta_2\xi_i p_{i,1}(t_j)\Theta_2\nu_i p_{i,1}(t_j)+T_N\Theta_2\nu_i p_{i,1}(t_j)+V_N\Theta_2\xi_i p_{i,1}(t_j)\right]$$
$$+\beta\Theta_2\mu_i p_{i,1}(t_j)+R_{2,N}(t_j),$$
$$F_{3,j}=\Theta_2\nu_i h_i(t_j)-N^*\beta\Theta_2\mu_i p_{i,1}(t_j)+\gamma\Theta_2\nu_i p_{i,1}(t_j)+R_{3,N}(t_j).$$

Broyden method is used for solution of above system. Jacobian is

$$\mathbf{J}=[J_{jk}]_{3M\times 3M}, \tag{23}$$

where

$$J_{jk}=\begin{cases}
\dfrac{\partial F_{1,j}}{\partial\xi_k}=h_k(t_j)+\alpha p_{k,1}(t_j)+k^*\left[p_{k,1}(t_j)\Theta_2\nu_i p_{i,1}(t_j)+V_N p_{k,1}(t_j)\right]\\
\qquad\qquad+\dfrac{r}{T_{\max}}\left[2\Theta_2\xi_i p_{i,1}(t_j)p_{k,1}(t_j)+p_{k,1}(t_j)\Theta_2 p_{i,1}(t_j)+I_N p_{k,1}(t_j)\right],\\
\dfrac{\partial F_{1,j}}{\partial\mu_k}=\dfrac{r}{T_{\max}}\left[\Theta_2\xi_i p_{i,1}(t_j)p_{k,1}(t_j)+T_N p_{k,1}(t_j)\right],\\
\dfrac{\partial F_{1,j}}{\partial\nu_k}=-k^*\left[\Theta_2 xi_i p_{i,1}(t_j)p_{k,1}(t_j)+T_N p_{k,1}(t_j)\right],\\
\dfrac{\partial F_{2,j}}{\partial\xi_k}=-k^*\left[p_{k,1}(t_j)\Theta_2\nu p_{k,1}(t_j)+V_N p_{k,1}(t_j)\right],\\
\dfrac{\partial F_{2,j}}{\partial\mu_k}=h_k(t_j)+\beta p_{k,1}(t_j),\\
\dfrac{\partial F_{2,j}}{\partial\nu_k}=-k^*\left[p_{k,1}(t_j)\Theta_2\xi_i p_{i,1}(t_j)+T_N p_{k,1}(t_j)\right],\\
\dfrac{\partial F_{3,j}}{\partial\xi_k}=0,\\
\dfrac{\partial F_{3,j}}{\partial\mu_k}=-N^*\beta p_{k,1}(t_j),\\
\dfrac{\partial F_{3,j}}{\partial\nu_k}=h_k(t_j)+\gamma p_{k,1}(t_j).
\end{cases}$$

The unknown coefficients ξ_i, μ_i and ν_i are obtained from the solution of this system. The approximate solution at discrete CPs is obtained by plugging ξ_i, ν_i ν_i $i = 1, 2, \ldots M$ in Eq. (22). Substituting the values of $e_{1,N,M}(t)$, $e_{2,N,M}(t)$ and $e_{3,N,M}(t)$ in system (16), we get the required solution.

5 Numerical Applications

The performance of the HWC technique is tested on example in this section. The numerical results are compared with Runge-Kutta technique, Bessel collocation technique, LADM-Pade and Galerkin technique available in the literature.

Problem 1. Consider the following system [5]

$$\begin{aligned}
\frac{dT}{dt} &= 0.1 - 0.02 + T\left(1 - \frac{T+I}{1500}\right) - 0.0027VT \\
\frac{dI}{dt} &= -0.0027VT - 0e.3I, \\
\frac{dV}{dt} &= 10(0.3)I - 2.4V,
\end{aligned} \tag{24}$$

with $T(0) = 0.1$, $I(0) = 0$ and $V(0) = 0.1$. The interval of study is $0 \leq t \leq 1$.

The first order derivatives $\frac{dT}{dt}$, $\frac{dI}{dt}$ and $\frac{dV}{dt}$ in above system (24) are approximated by Haar functions. Let $\frac{dT}{dt}$, $\frac{dI}{dt}$ and $\frac{dV}{dt}$ are square integrable functions then

$$\frac{dT(t)}{dt} = \Theta_1 a_i h_i(t), \quad \frac{dI(t)}{dt} = \Theta_1 b_i h_i(t) \quad \text{and} \quad \frac{dV(t)}{dt} = \Theta_1 c_i h_i(t). \tag{25}$$

By using initial conditions and integration, we obtain the approximate solution of this system in terms of Haar functions

$$T(t) = 0.1 + \Theta_1 a_i p_{i,1}(t), \quad I(t) = \Theta_1 b_i p_{i,1}(t), \quad \text{and} \quad V(t) = 0.1 + \Theta_1 c_i p_{i,1}(t). \tag{26}$$

Putting these approximations and CPs in above system (24), we obtain a system of nonlinear algebraic equations which is then solved by the method of Broyden's. Error estimation is also calculated in a similar way, which aims to reduce the error of numerical solution. The residual functions $R_{1,N}(t)$, $R_{2,N}(t)$ and $R_{3,N}(t)$ are calculated as discussed in Eq. (14). The errors functions $e_{1,N}(t)$, $e_{2,N}(t)$, and $e_{3,N}(t)$ are obtained as discussed in Eq. (15).

The error functions for distinct CPs and distinct values of time are given in Tables 1–3. The error functions obtained for variable $N = 3$ at different values of t are compared with Laplace Adomian decomposition technique, Runge-Kutta technique, modified variational iteration technique, Pade approximation, the perturbation-iteration algorithm, Bessel collocation technique, differential transform technique and exponential Galerkin technique available in literature. From the tables we see that as N increases, the values of our results near to those of the other techniques. This show that our approximate solution become accurate as the number of discrete CPs N increases. Even a batter accuracy is obtained by taking more discrete CPs. The graph of numerical solution is also given in Fig. 1. The estimated results of error functions for distinct number of CPs are shown in Fig. 2. Due to the simplicity of the Haar wavelet it is effective for solution of the first-order of HIV infection $CD4^+$ T-Cells model. However, HWC scheme has disadvantages too. This method use constant box functions and due to this we need a large number of collocation points in order to achieve better accuracy. This disadvantage can

be overcome if Haar wavelet is replaced with some other wavelets having better approximating properties.

Table 1: Comparison for uninfected cells $T(t)$

t	Runge-Kutta	LADM-Pade [1]	Bessel coll. $N=8$ [2]	PIA(1,1) [3]	MVIM [4]
0.2	0.2087297222	0.2088072731	0.2038616561	0.2087295073	0.2088080868
0.4	0.4059409955	0.4061052625	0.3803309335	0.4059404993	0.4062407949
0.6	0.7635801781	0.7611467713	0.6954623767	0.7635790156	0.7644287245
0.8	1.4119574363	1.3773198590	1.2759624442	1.4119543417	1.4140941730
1.0	2.5867778755	2.3291697610	2.3832277428	2.5867690583	2.5919210760
t	DTM $N=6$ [7]	Galerkin technique $N=3$ [5]	Galerkin technique $N=4$ [5]	Galerkin technique $N=5$ [5]	Our solution $N=3$ (HWC method)
0.2	0.211648	0.2722229510	0.2345157340	0.1982953765	0.2073431784
0.4	0.422685	0.3065308713	0.4201803666	0.4183153468	0.3930921357
0.6	0.817940	0.7075440591	0.7255920466	0.7603331972	0.6453087042
0.8	1.546211	1.5297610198	1.4170402360	1.4077147917	1.3978540981
1.0	2.854053	2.6678673734	2.5916251711	2.5915947135	2.5709802316
t	Present technique $N=3$ (Results of errors)				
0.2	3.336883e–004				
0.4	3.373781e–004				
0.6	2.869852e–003				
0.8	1.341768e–003				
1.0	1.130869e–002				

Table 2: Comparison for infected $I(t)$

t	Runge-Kutta	LADM-Pade [1]	Bessel coll. $N=8$ [2]	PIA(1,1) [3]	MVIM [4]
0.2	0.0000060315	0.0000060327	0.0000062478	0.0000060315	0.0000060327
0.4	0.0000131530	0.0000131591	0.0000129355	0.0000131530	0.0000131583
0.6	0.0000212106	0.0000212683	0.0000203526	0.0000212101	0.0000212233
0.8	0.0000301518	0.0000300691	0.0000283730	0.0000301480	0.0000301745
1.0	0.0000399942	0.0000398736	0.0000369084	0.0000399785	0.0000400254
t	DTM $N=6$ [7]	Galerkin technique $N=3$ [5]	Galerkin technique $N=4$ [5]	Galerkin technique $N=5$ [5]	Our solution $N=3$ (HWC method)

(Continued)

Table 2 (continued)

0.2	0.0000063666	0.0000091673	0.0000058251	0.0000059641	0.0000070416
0.4	0.0000139924	0.0000155229	0.0000134051	0.0000131340	0.0000140251
0.6	0.0000226514	0.0000228459	0.0000213405	0.0000212682	0.0000230126
0.8	0.0000332836	0.0000318486	0.0000301313	0.0000301754	0.0000309231
1.0	0.0000485399	0.0000421057	0.0000400369	0.0000400377	0.0000403894

t	Present technique $N = 3$ (Results of errors)
0.2	1.688238e–008
0.4	1.754047e–008
0.6	1.732461e–006
0.8	1.865676e–006
1.0	1.961419e–006

Table 3: Comparison for free virus particles $V(t)$

t	Runge-Kutta	LADM-Pade [1]	Bessel coll. $N = 8$ [2]	PIA(1,1) [3]	MVIM [4]
0.2	0.0618798121	0.0618799602	0.0618799185	0.0618796999	0.0618799087
0.4	0.0382948730	0.0383132488	0.0382949349	0.0382939096	0.0382959576
0.6	0.0237045402	0.0243917434	0.0237043186	0.0237016917	0.0237102948
0.8	0.0146803506	0.0099672189	0.0146795698	0.0146744145	0.0147004190
1.0	0.0091008270	0.0033050764	0.0090993030	0.0090905052	0.0091572387

t	DTM $N = 6$ [7]	Galerkin technique $N = 3$ [5]	Galerkin technique $N = 4$ [5]	Galerkin technique $N = 5$ [5]	Our solution $N = 3$ (HWC method)
0.2	0.061880	0.0618823466	0.0618790041	0.0618799035	0.0617912741
0.4	0.038309	0.0383077329	0.0382950148	0.0382947890	0.0380026874
0.6	0.023920	0.0237055266	0.0237053683	0.0237046061	0.0236011879
0.8	0.016212	0.0146708169	0.0146798882	0.0146803810	0.0139672890
1.0	0.016050	0.0091056907	0.0091009339	0.0091008486	0.0089053621

t	Present technique $N = 3$ (Results of errors)
0.2	1.421018e–014
0.4	1.854715e–014
0.6	1.908546e–014
0.8	2.842172e–014
1.0	2.943048e–014

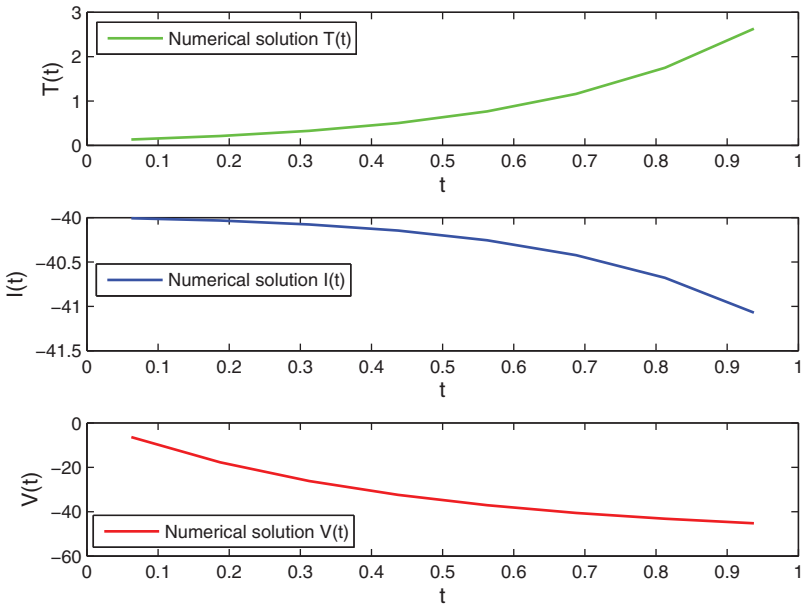

Figure 1: Numerical solution of problem 1

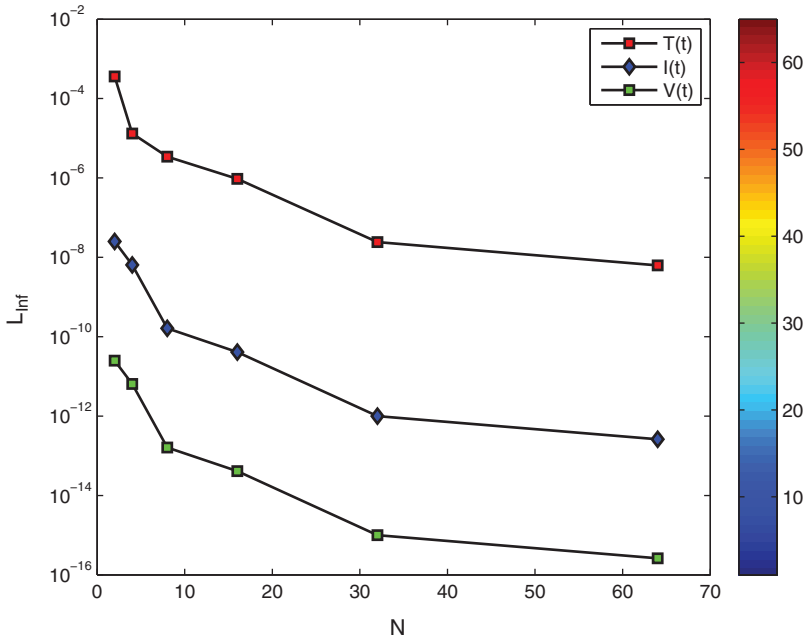

Figure 2: Estimated error functions for problem 1

6 Conclusion

Haar collocation scheme is developed for the solution of the HIV CD4$^+$ T-cells model. Also, we discussed a procedure known as residual error estimation, whose aim is to get better arrangements utilizing the obtained solution. The technique is tested on one example, and the results are compared with other methods available in the literature. The comparison of the present HWC technique with Runge-Kutta technique, Bessel collocation technique, LADM-Pade and Galerkin

technique is given. The results demonstrate that Haar technique is effective and precise for distinct numbers of CPs. The results show that taking the large value of variable N, the HWC technique give the accurate results of the numerical solution. The error functions using various numbers of CPs are also calculated and reported in the table. From results, it is seen that proposed technique gives good results for this model. The proposed technique is easily implemented in any software packages. MATLAB software is used to obtain the numerical results.

Acknowledgement: The authors are very grateful to the anonymous referees for their constructive comments which have improved the paper.

Funding Statement: No funding is available to support this study.

Conflicts of Interest: On behalf of all authors, the corresponding author states that there is no conflict of interest.

References

1. Ongun, M. Y. (2011). The laplace adomian decomposition method for solving a model for HIV infection of $CD4^+$ T cells. *Mathematical and Computer Modelling, 53,* 597–603. DOI 10.1016/j.mcm.2010.09.009.
2. Yuzbasi, S. (2012). A numerical approach to solve the model for HIV infection of $CD4^+$ T cells. *Applied Mathematical Modelling, 36,* 5876–5890. DOI 10.1016/j.apm.2011.12.021.
3. Khalid, M., Sultana, M., Zaidi, F., Fareeha, S. K. (2015). A numerical solution of a model for HIV infection $CD4^+$ T-cell. *International Journal of Innovation Science and Research, 16(1),* 79–85. DOI 10.1.1.1010.9251.
4. Merdan, M., Gokdogan, A., Yildirim, A. (2011). On the numerical solution of the model for HIV infection of $CD4^+$ T cells. *Computers and Mathematics with Applications, 62(1),* 118–123. DOI 10.1016/j.camwa.2011.04.058.
5. Yuzbasi, S., Karacayir, M. (2017). An exponential galerkin method for solutions of HIV infection model of $CD4^+$ T-cells. *Computational Biology and Chemistry, 67,* 205–212. DOI 10.1016/j.compbiolchem.2016.12.006.
6. Nelson, P. W., Perelson, A. S. (2002). Mathematical analysis of delay differential equation models of HIV-1 infection. *Mathematical Biosciences, 179,* 73–94. DOI 10.1016/S0025-5564(02)00099-8.
7. Srivastava, V. K., Awasthi, M. K., Kumar, S. (2014). Numerical approximation for HIV infection of $CD4^+$ T cells mathematical model. *Ain Shams Engineering Journal, 5,* 625–629. DOI 10.1016/j.asej.2013.12.012.
8. Lane, H. C., Fauci, A. (1985). Immunologic abnormalities in the acquired immunodeficiency syndrome. *Annual Review of Immunology, 3(1),* 77–500. DOI 10.1146/annurev.iy.03.040185.002401.
9. Perelson, A. S. (1989). Modeling the interaction of the immune system with HIV. In: *Mathematical and statistical approaches to AIDS epidemiology*, vol. 83, pp. 350–370. Berlin, Heidelberg: Springer. DOI 10.1007/978-3-642-93454-4_17.
10. Culshaw, R. V., Ruan, S. (2000). A delay-differential model of HIV infection of $CD4^+$ T-cells. *Mathematical Biosciences, 165(1),* 27–39. DOI 10.1016/S0025-5564(00)00006-7.
11. Merdan, M. (2007). Homotopy perturbation method for solving a model for HIV infection of $CD4^+$ T-cells. *Istanbul Ticaret Universitesi Fen Bilimleri Dergisi, 12,* 39–52.
12. Wang, L., Li, M. Y. (2006). Mathematical analysis of the global dynamics of a model for HIV infection of $CD4^+$ T cells. *Mathematical Biosciences, 200(1),* 44–57. DOI 10.1016/j.mbs.2005.12.026.
13. Elaiw, A. M., Alsheri, A. (2013). Global dynamics of HIV infection of $CD4^+$ T cells and macrophages. *Discrete Dynamics in Nature and Society, 2013,* 1–9. DOI 10.1155/2013/264759.
14. Ullah, R., Ellahi, R., Sait, S. M., Mohyud-Din, S. T. (2020). On the fractional-order model of HIV-1 infection of $CD4^+$ T-cells under the influence of antiviral drug treatment. *Journal of Taibah University for Science, 14(1),* 50–59. DOI 10.1080/16583655.2019.1700676.

15. Yüzbas, S., Yldrm, G. (2020). Pell–lucas collocation method for numerical solutions of two population models and residual correction. *Journal of Taibah University for Science, 14(1),* 1262–1278. DOI 10.1080/16583655.2020.1816027.
16. Mallawi, F., Alzaidy, J., Hafez, R. (2019). Application of a legendre collocation method to the space–time variable fractional-order advection–dispersion equation. *Journal of Taibah University for Science, 13(1),* 324–330. DOI 10.1080/16583655.2019.1576265.
17. Yüzbas, S. (2020). An operational method for solutions of riccati type differential equations with functional arguments. *Journal of Taibah University for Science, 14(1),* 661–669. DOI 10.1080/16583655.2020.1761661.
18. Chu, Y., Khater, M. M. A., Hamed, Y. S. (2021). Diverse novel analytical and semi-analytical wave solutions of the generalized (2 + 1)-dimensional shallow water waves model. *AIP Advances, 11,* 015223. DOI 10.1063/5.0036261.
19. Khater, M. M. A., Ahmed, A. E., El-Shorbagy, M. (2021). Abundant stable computational solutions of atangana baleanu fractional nonlinear HIV-1 infection of $CD4^+$ T-cells of immunodeficiency syndrome. *Results in Physics, 22,* 103890. DOI 10.1016/j.rinp.2021.103890.
20. Khater, M. M. A., Mohamed, M. S., Attia, R. A. (2021). On semi analytical and numerical simulations for a mathematical biological model; the time-fractional nonlinear Kolmogorov–Petrovskii–Piskunov (KPP) equation. *Chaos. Solitons and Fractals, 144,* 110676. DOI 10.1016/j.chaos.2021.110676.
21. Khater, M. M. A., Ahmed, A. E., Alfalqi, S. H., Alzaidi, J. F., Elbendary, S. et al. (2021). Computational and approximate solutions of complex nonlinear fokas–lenells equation arising in optical fiber. *Results in Physics, 25,* 104322. DOI 10.1016/j.rinp.2021.104322.
22. Khater, M. M. A., Mousa, A. A., El-Shorbagy, M. A., Attia, R. A. M. (2021). Analytical and semi-analytical solutions for phi-four equation through three recent schemes. *Results in Physics, 22,* 103954. DOI 10.1016/j.rinp.2021.103954.
23. Khater, M. M. A., Nisar, K. S., Mohamed, M. S. (2021). Numerical investigation for the fractional nonlinear space-time telegraph equation via the trigonometric quintic b-spline scheme. *Mathematical Methods in Applied Sciences, 44,* 4598–4606. DOI 10.1002/mma.7052.
24. Khater, M. M. A., Nofal, T. A., Zinadah, H. A., Lotayif, M. S. M., Lu, D. (2021). Novel computational and accurate numerical solutions of the modified benjamin bona mahony (bbm) equation arising in the optical illusions field. *Alexandria Engineering Journal, 60,* 1797–1806. DOI 10.1016/j.aej.2020.11.028.
25. Khater, M. M. A., Mohamed, M. S., Elagan, S. (2021). Diverse accurate computational solutions of the nonlinear klein fock gordon equation. *Results in Physics, 23,* 104003. DOI 10.1016/j.rinp.2021.104003.
26. Khater, M. M. A., Bekir, A., Lu, D., Attia, R. A. M. (2021). Analytical and semi analytical solutions for time-fractional cahn allen equation. *Mathematical Methods in Applied Sciences, 44,* 2682–2691. DOI 10.1002/mma.6951.
27. Khater, M. M. A., Elagan, S. K., Mousa, A. A., El-Shorbagy, M. A. et al. (2021). Sub-10-fs-pulse propagation between analytical and numerical investigation. *Results in Physics, 25,* 104133. DOI 10.1016/j.rinp.2021.104133.
28. Attia, R. A. M., Khater, M. M. A., Ahmed, A. E., El-Shorbagy, M. A. (2021). Accurate sets of solitary solutions for the quadratic–cubic fractional nonlinear schrödinger equation. *AIP Advances, 11,* 055105. DOI 10.1063/5.0050624.
29. Khater, M. M. A., Ahmed, A. E. (2021). Strong langmuir turbulence dynamics through the trigonometric quintic and exponential B-spline schemes. *AIMS Mathematics, 6,* 5896–5908. DOI 10.3934/math.2021349.
30. Yue, C., Lu, D., Khater, M. M. A. (2021). Abundant wave accurate analytical solutions of the fractional nonlinear hirota–satsuma–shallowwater wave equation. *Fluids, 6,* 235. DOI 10.3390/fluids6070235.
31. Khater, M. M. A., Alabdali, A. M. (2019). Multiple novels and accurate traveling wave and numerical solutions of the (2 + 1) dimensional fisher-kolmogorov-petrovskii-piskunov equation. *Mathematics, 9,* 1440. DOI 10.3390/math9121440.
32. Li, W., Akinyemi, L., Lu, D., Khater, M. M. A. (2021). Abundant traveling wave and numerical solutions of weakly dispersive long waves model. *Symmetry, 13,* 1085. DOI 10.3390/sym13061085.

33. AL-Smadi, M. H., Gumah, G. N. (2014). On the homotopy analysis method for fractional seir epidemic model. *Research Journal of Applied Sciences*, *Engineering and Technology, 18(7),* 3809–3820. DOI org//10.19026/rjaset.7.738.
34. Freihet, A., Hasan, S., Al-Smadi, M., Gaith, M., Momani, S. (2019). Construction of fractional power series solutions to fractional stiff system using residual functions algorithm. *Advances in Difference Equations, 95,* 1–15. DOI 10.1186/s13662-019-2042-3.
35. Al-Smadi, M., Arqub, O. A., Hadid, S. (2020). An attractive analytical technique for coupled system of fractional partial differential equations in shallow water waves with conformable derivative. *Communications in Theoretical Physics, 72,* 085001. DOI 10.1088/1572-9494/ab8a29.
36. Al-Smadi, M., Arqub, O. A., Hadid, S. (2020). Approximate solutions of nonlinear fractional kundu-eckhaus and coupled fractional massive thirring equations emerging in quantum field theory using conformable residual power series method. *Physica Scripta, 95,* 105205. DOI 10.1088/1402-4896/abb420.
37. Al-Smadi, M., Arqub, O. A., Momani, S. (2020). Numerical computations of coupled fractional resonant schrödinger equations arising in quantum mechanics under conformable fractional derivative sense. *Physica Scripta, 95,* 075218. DOI 10.1088/1402-4896/ab96e0.
38. Al-Smadi, M. (2021). Fractional residual series for conformable time-fractional Sawada–Kotera–Ito, Lax, and Kaup–Kupershmidt equations of seventh order. *Mathematical Methods in Applied Sciences,* 1–22. DOI 10.1002/mma.7507.
39. Al-Smadi, M., Arqub, O. A., Zeidan, D. (2021). Fuzzy fractional differential equations under the mittag-leffler kernel differential operator of the abc approach: Theorems and applications. *Chaos*, *Solitons and Fractals, 146,* 110891. DOI 10.1016/j.chaos.2021.110891.
40. Aziz, I., Amin, R. (2016). Numerical solution of a class of delay differential and delay partial differential equations via Haar wavelet. *Applied Mathematical Modelling, 40,* 10286–10299. DOI 10.1016/j.apm.2016.07.018.
41. Amin, R., Nazir, S., Magrino, I. G. (2020). A collocation method for numerical solution of nonlinear delay integro-differential equations for wireless sensor network and internet of things. *Sensors, 20,* 1962–1973. DOI 10.3390/s20071962.
42. Amin, R., Nazir, S., Magrino, I. G. (2019). Efficient sustainable algorithm for numerical solution of nonlinear delay Fredholm-Volterra integral equations via Haar wavelet for dense sensor networks in emerging telecommunications. *Transactions on Emerging Telecommunications Technologies, 30(11),* 1–12. DOI org//10.1002/ett.3877.
43. Nazir, S., Shahzad, S., Wirza, R., Amin, R., Ahsan, M. et al. (2019). Birthmark based identification of software piracy using Haar wavelet. *Mathematics and Computers in Simulation, 166,* 144–154. DOI 10.1016/j.matcom.2019.04.010.
44. Khashan, M. M., Amin, R., Syam, M. I. (2019). A new algorithm for fractional riccati type differential equations by using Haar wavelet. *Mathematics, 7,* 545–557. DOI 10.3390/math7060545.
45. Amin, R., Shah, K., Asif, M., Khan, I., Ullah, F. (2021). An efficient algorithm for numerical solution of fractional integro-differential equations via Haar wavelet. *Journal of Computational and Applied Mathematics, 381,* 113028. DOI 10.1016/j.cam.2020.113028.
46. Abdeljawad, T., Amin, R., Shah, K., Mdallal, Q., Jarad, F. (2020). Efficient sustainable algorithm for numerical solutions of systems of fractional order differential equations by Haar wavelet collocation method. *Alexandria Engineering Journal, 59,* 2391–2400. DOI 10.1016/j.aej.2020.02.035.
47. Amin, R., Ahmad, H., Shah, K., Hafeez, M. B., Sumelka, W. (2021). Theoretical and computational analysis of nonlinear fractional integro-differential equations via collocation method. *Chaos*, *Solitons and Fractals, 151,* 111252. DOI 10.1016/j.chaos.2021.111252.